Jestr

Journal of Engineering Science and Technology Review 9 (6) (2016) 82- 86

Research Article

JOURNAL OF
Engineering Science and Technology Review

www.jestr.org

An Accurate Approach of Mathematical Modeling of SRR and SR for Metamaterials

Rajni[1,*] and Anupma Marwaha[2]

[1]*Department of Electronics and Communication Engineering, Shaheed Bhagat Singh State Technical Campus, Ferozepur, Punjab 152004, India*
[2]*Department of Electronics and Communication Engineering, Sant Longowal Institute of Engineering and Technology, Longowal, Sangrur, Punjab 148106, India*

Received 1 August 2016; Accepted 13 December 2016

Abstract

In the proposed work, we used two miniaturized resonant inclusions, spiral resonators (SRs) and split ring resonators (SRRs) used in practical implementation of metamaterials. A spiral resonator is modeled on a Rogers's duroid substrate of permittivity 2.2. This structure is numerically analysed inside a rectangular waveguide with electromagnetic solver. A full wave simulation of a double split ring resonator with same design parameters is performed inside a waveguide. The transmission minimum frequency of SR is evaluated for varying number of turns in SR where as it is accessed for varying number of rings in SRRs. The full wave simulated transmission minimum frequency is compared with frequency derived from equivalent circuit model of each respective model. In this paper, the expressions derived for resonant frequency are simplified for evaluating effective dielectric constant of substrate after incorporation of metallic inclusion. It is found that the analytically calculated resonant frequency is in close agreement with full wave numerically analyzed frequency. It is also confirmed that SR decrease the electrical dimensions of the resonant inclusions to a great extent as compared to SRR, while synthesizing artificial metamaterials.

Keywords: Metamaterials; Left-Handed Materials; Spiral Resonator; Split Ring Resonator; High Frequency Simulation Software

1. Introduction

Although the research for 'synthetic' materials was initiated in 1948 for microwave applications [1] yet metamaterials (MTM) emerged as a breakthrough in the field of electromagnetic since last decade only. Metamaterials have fascinated vast interest due to their unique responses to electromagnetic radiations, which are generally not encountered in their natural forms [2-3]. These materials are engineered by embedding precise metallic inclusions or inhomogeneties in host media like substrate at microwave frequencies. The special feature of MTM is that these owe their properties from their structure and not inherit from chemical composition of their constituents.

The novel concept of metamaterials was given by Victor Veselago in 1968 who stated that Poynting vector of a monochromatic plane wave will flow in anti-parallel to its phase velocity in a medium having dielectric permittivity (ε) and magnetic permeability(μ), to be simultaneous negative [4]. He named these materials as "Left-Handed Materials" (LHM). In 1999, J.B. Pendry proposed that realization of artificial negative permeability medium by employing an array of minute resonant metallic inclusions called as split ring resonators (SRR) [5]. In 2000, a LHM structure consisted of aligned wire medium to depict the epsilon negative (ENG) properties [6], and resonant loop inclusions, termed as split-ring resonators to get negative (MNG) features, was used for the first time [7] to demonstrate the negative electromagnetic features. The size of the inclusions should be less than the operating wavelength. Multiple splits [8] and modified geometries for SRR geometry are introduced in [9-10] tailoring the tuning of resonant frequency. An equivalent LC resonant circuit represents the electromagnetic field interaction of the inclusions. The equivalent circuit model for geometries of SRRs is presented in [11].

The inadequate available lithographic techniques have restricted the researchers to exceed dimensions of the inclusions beyond sub-wavelength. Various structures of rings e.g. square-shaped, circular, U-shaped, spiral and S-shaped etc. are used and analyzed in [12-16] to form new MTMs. New MTMs using triangular shaped rings are reported by C. Sabah [17] which have not been studied before 2008. The effective medium metamaterial substrate, engineered through metallic inclusions, can achieve enhanced permeability and permittivity as compared to the host dielectric employed without inclusions. According to [18-19], the geometry of metallic inclusions customized to the application can control the effective parameters of the substrate. Bilotti et al. derived new analytical design formulas for both MSRRs and SRs on the basis of quasi-static model and compared with the previous formulas and numerical analysed results [20]. Ellstein et al. derived analytical circuit models for a single layer and a double layer spiral resonators models and showed through experimental measurements and numerical simulations that these models are more accurate to previous circuit models [21]. If equivalent circuit is considered, no paper suggests a very accurate design formula for magnetic inclusion. The authors in [22] reported that distributed capacitance associated between the rings of SRR or turns of SR is affected by dielectric properties, but inductance does not depend upon it.

* E-mail address: rajni_c123@yahoo.co.in

In this paper, we analyzed modified mathematical model of equivalent circuit of the SRR and SR with varying number of rings/ turns and showed that analytical results nearly match with its full-wave numerical simulations results. A square inductive loop structure has been preferred in a number of previous designs in literature. The use of SR's is proposed in this paper as it has the potential to decrease the size of MTM electrically than the square SRR structures. This paper is organised in four sections. Section 1 describes brief introduction and history of work done in the same area. Section 2 gives the design of resonators. Section 3 presents the simulation methodology. Section 4 presents and discusses results. Section 5 concludes the paper.

2. Design and Modeling the Circuits of Resonators

2.1. Spiral Resonators

First, we considered SR of two turns with length of Outer turn as 4 mm shown in Figure 1(a). The gap (g) of SR is 0.2 mm, the strip width (t) and substrate thickness (h) is 2 mm. The spacing(s) between nth and (n+1) turn is 0.2 mm. The SR is mounted on a Rogers's duroid 5880 tm substrate having relative permittivity ε_r as 2.2, and loss tangent 0.0009. The quasi-static equivalent circuit of SR is depicted in Figure 1(b).

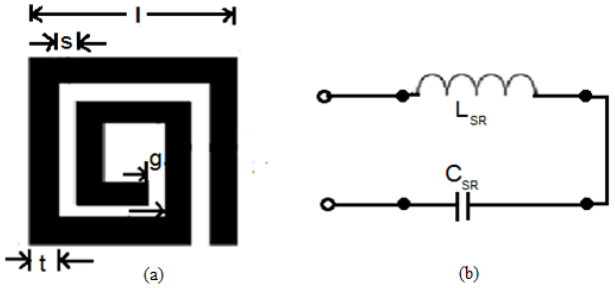

Fig. 1. (a) Geometry of SR with no. of turns (N) = 2; (b) Equivalent Circuit Diagram of SR.

The inductance, L_{SR} of the tank circuit model is calculated by assuming uniform current throughout the spiral. The capacitance, C_{SR} of the tank circuit is assumed to be the parallel equivalent of the capacitances corresponding to each pair of adjacent loops. The tank circuit model deduces that the SR has only a single resonant frequency. SR has metallic strip of width *'t'* and separation *'s'* between two consecutive turns. The value of L_{SR} and of the distributed capacitance of SR can be derived found by calculating total length of strip l_n of the general nth turn of the spiral and total length l_n^g of the gap between nth and (n+1)th turns of the spiral.

$$l_n = \{\, 4[l - (n(t+s)]\,,\ n > 1 \tag{1}$$

$$l_n^g = \left\{ \frac{l_n + l_{n+1}}{2} \right. = 4\left[l - \left(n + \frac{1}{2}\right)(t+s)\right],\ n > 1 \tag{2}$$

Here l is the length of outermost turn and the distributed capacitances is the capacitance among two consecutive turns of spiral connected in parallel, so the total distributed capacitance, C_{sr} for total no. of turns N will be given by

$$C_{sr} = \sum_{n=1}^{N-1} C_{n(n+1)}^t \tag{3}$$

$C_{n(n+1)}^t$ is distributive capacitance between n and n+1 turn and is expressed as

$$C_{n(n+1)}^t = l_n^g C_{pul} \tag{4}$$

C_{pul} is per unit length capacitance of two parallel strips of width *'t'* apart by distance *'s'*. The dielectric substrate has an effect on the distributed capacitance only and is given by

$$C_{pul} = \varepsilon_o \varepsilon_{rdc} \frac{K\left(\sqrt{1-k^2}\right)}{K(k)} \tag{5}$$

ε_0 is dielectric constant of free space, ε_r is relative permeability of substrate and ε_{rdc} is relative effective permittivity or dielectric constant of substrate due to metallic inclusions and depend on height, relative permittivity of substrate, width of parallel plates and spacing between them. Authors in [22] have given a relationship between ε_r, relative permittivity of substrate and ε_{rdc}, relative effective permittivity or dielectric constant of substrate due to metallic inclusions. But in this paper this equation has been simplified for parameters taken and is given by equation as follows [21]:

$$\varepsilon_{rdc} = 1 + \varepsilon_r/2 \tag{6}$$

$K(k)$ is known as the complete elliptical integral of the first kind, and $k = s/(s+2t)$. The total distributed capacitance is given by

$$C_{sr} = 4C_{pul} \sum_{n=1}^{N-1} \left[l - \left(n + \frac{1}{2}\right)(t+s)\right] \tag{7}$$

A correction factor C_f should be added to equation (8) to compensate the mutual interactions between non-consecutive turns [22]. The correction factor depends upon number of turns per unit length.
C_{SR} of the equivalent circuit is given by

$$C_{SR} = C_{sr} * C_f \tag{8}$$

$$\text{Correction factor, } C_f = \frac{l}{16(t+s)} * \frac{N^2}{(N^2+1)} \tag{9}$$

Putting value of equation (7) in equation (9)

$$C_{SR} = \varepsilon_{rdc} \frac{l}{4(t+s)} * \frac{N^2}{(N^2+1)} \sum_{n=1}^{N-1} \left[l - \left(n + \frac{1}{2}\right)(t+s)\right] \tag{10}$$

$$l_{avg}^{SR} = \frac{1}{N} \sum_{n=1}^{N} l_n = \frac{4lN - [2N(1+N) - 3](s+t)}{N} \tag{11}$$

The presence of a dielectric substrate does not have an effect on the inductance. So it is given by

$$L_{SR} = \frac{\mu_0}{2\pi} l_{avg}^{SR} \left[\frac{1}{2} + \ln\left(\frac{l_{avg}^{SR}}{2t}\right)\right] \tag{12}$$

Based on the above equations, the equivalent circuit component values can be calculated depending on the geometry, layout and material of the spiral. Once the circuit component values are obtained, they can be used for resonant frequency, f_r calculations.

$$f_r = \frac{1}{2\pi\sqrt{L_{SR} C_{SR}}} \tag{13}$$

2.2. Split Ring Resonators

We considered SRR with no. of rings N=2 with length of Outer ring as 4 mm as shown in Figure 2(a). The split or gap (g) of SR is 0.2 mm wide, the strip width (t) and substrate thickness (h) is 2 mm. The spacing(s) between nth and (n+1) turn is 0.2 mm. The SRR is mounted on a Rogers's duroid 5880 tm substrate having relative permittivity, ε_r as 2.2.

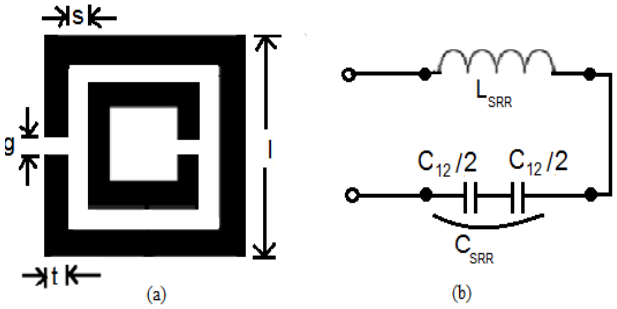

Fig. 2. (a) Geometry of SRR with no. of turns (N) = 2; (b) Equivalent Circuit Diagram of SRR.

Figure 2(a) shows the geometry of the SRR consisting of two rings with their slit displaced by 180° or 2π. The quasi-static equivalent circuit for SRR is presented in Figure 2(b). The inductance of the tank circuit model, L_{SRR} is calculated by assuming is uniform current throughout the loop. The capacitance of the tank circuit, C_{SRR} is assumed to be the parallel equivalent of the capacitances corresponding to each pair of adjacent loops. The total strip length, l_n of nth ring of the SRR and the total length, l_n^g of the gap between nth and (n+1)th turns of SRR are determined. Then the total inductance and of the total distributed capacitance between two consecutive rings of SRR, of strip width,t and separation, s between rings are derived.

$$l_n = 4[l - 2t(n-1) - 2s(n-1)] \tag{14}$$

$$l_n^g = \begin{cases} \frac{l_n + l_{n+1}}{2} \\ = 4\left[l - \left(n + \frac{1}{2}\right)(t+s)\right], \ n > 1 \end{cases} \tag{15}$$

l is the length of the outermost ring, total distributed capacitance, C_{SRR}, due to (n-1) capacitances connected in parallel due to spacing amid two consecutive rings, will be given by

$$C_{SRR} = \sum_{n=1}^{N-1} \frac{C_{n(n+1)}}{4} \tag{16}$$

$$C_{SRR} = \frac{N-1}{2}[2l - (2N-1)(t+s)]C_{pul} \tag{17}$$

N is no. of rings, $C_{n(n+1)}/4$ is series between two equal valued distributive capacitances, $C_{n(n+1)}/2$ between two halves of nth and (n+1)th rings. The total distributed capacitance $C_{n(n+1)}$between rings is explained as

$$C_{n(n+1)} = [l_{n+1} + 2(t+s)]C_{pul} \tag{18}$$

C_{pul} is per unit length capacitance between two parallel strips. It is already mentioned that the distributed capacitance get varied with dielectric substrate height and dielectric constant.

Putting the value of $C_{pul}$from equations (5) and (6) in equation (17),

$$C_{SRR} = \frac{N-1}{2}[2l - (2N-1)(t+s)][\varepsilon_o(1+\varepsilon_r)/2]\frac{K(\sqrt{1-k^2})}{K(k)} \tag{19}$$

$$l_{avg} = \frac{1}{N}\sum_{n=1}^{N} l_n = 4[l - (N-1)(s+t)] \tag{20}$$

The dielectric substrate properties, upon which resonators are printed has no affect on the inductance. Therefore, its expression is given by

$$L_{SRR} = \frac{\mu_0}{2}\frac{l_{avg}}{4}\, 4.86\left[\ln\left(\frac{0.98}{\rho}\right) + 1.84\rho\right] \tag{21}$$

where ρ is fill ratio of SRR and is given by

$$\rho = \frac{(N-1)(s+t)}{l-(N-1)(s+t)} \tag{22}$$

By putting equation (20) in (22), L_{SRR} is given by

$$L_{SRR} = \frac{\mu_0}{2}[l - (N-1)(s+t)]4.86\left[\ln\left(\frac{0.98}{\rho}\right) + 1.84\rho\right] \tag{23}$$

Based on the above equations, the equivalent circuit component values can be calculated depending on the geometry, layout and material of the spiral. Once the circuit component values are obtained, they can be used to for resonant frequency f_r calculations.

$$f_r = \frac{1}{2\pi\sqrt{L_{SRR}C_{SRR}}} \tag{24}$$

3. Simulation Methodology

To reveal the metamaterial properties in the preferred working frequency region, First SR unit cell with varying number of turns is numerically analyzed using High frequency simulation software (HFSS) in a rectangular waveguide. Subsequently, SRR with varying number of rings is simulated in waveguide. For this, perfect electric conductor boundary conditions are employed on in x direction and the perfect magnetic conductor boundary conditions are applied in z direction on unit cell. The two wave ports 1 and 2 are assigned along each of the substrate line in y direction to excite the negative permeability behavior of resonators as shown in Figure 3.

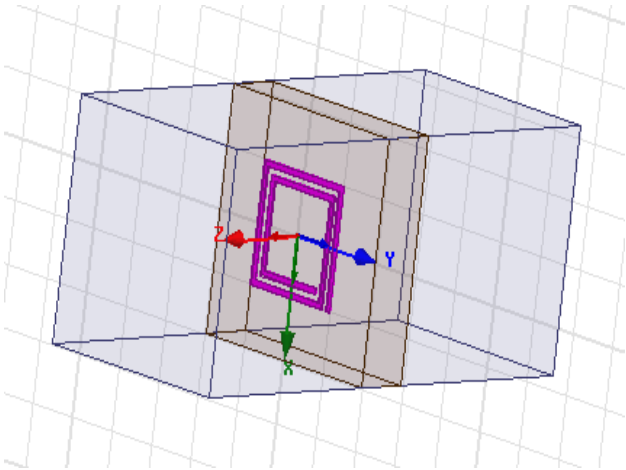

Fig. 3. SR structure in waveguide.

4. Results and Discussion

4.1. Simulated Results of SR

First SR structure is simulated with in waveguide. A triad of E, H, and k is generated to reveal electromagnetic propagation through the structure. This numerical method derives resonant frequency quite accurately. We can observe the transmission minimum frequency of resonant particle with varying number of turns (N) of spiral as 2, 3, 4, 5 and 6. The effect of variation of number of turns on resonating frequency thus observed is depicted in Figure 4.

The values of inductance and capacitance in SR are computed to further calculate the transmission minimum frequency. Then the comparative analysis of calculated transmission minimum frequency with simulated frequency in case of SR is presented in Table 1.

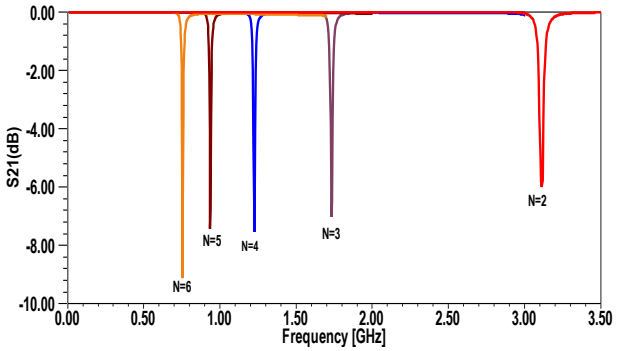

Fig. 4. Transmission minimum frequency with varying number of turns in SR.

Table 1. Calculated transmission minimum frequency and simulated frequency of SR.

S.No.	No. of turns (N)	Length of outer turn (*l*) (mm)	L(nH)	C(pF)	Transmission Minimum frequency (in GHz) (calculated)	Transmission Minimum frequency (in GHz) (simulated)
1	2	4	11.5575	0.189	3.41	3.107
2	3	4.8	13.821	0.600	1.667	1.730
3	4	5.6	16.2496	1.264	1.11	1.229
4	5	6.4	18.779	2.224	0.778	0.938
5	6	7.2	21.383	3.530	0.576	0.754

4.2. Simulated Results of SRR

SRR structure is simulated with in waveguide similar to SR. The three mutually perpendicular vectors E, H, and k are set on appropriate faces and excitation is applied to reveal electromagnetic propagation through the structure. After simulation, we can observe the transmission minimum frequency of resonant particle with varying number of rings (N) of SRR as 2,3,4,5 and 6. The resonating frequency thus observed is shown in Figure 5.

Also the values of inductance and capacitance in SRR are calculated to evaluate the transmission minimum frequency. The comparative analysis of calculated transmission minimum frequency with simulated frequency in case of SRR is presented in Table 2.

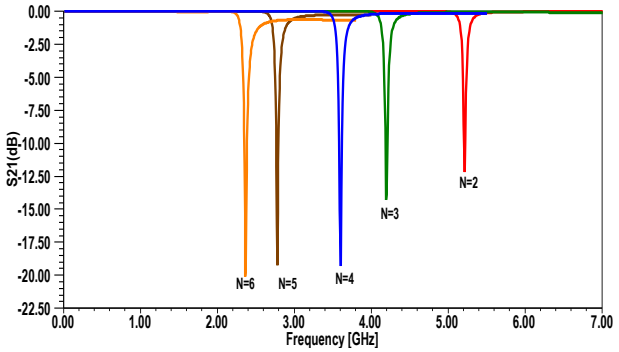

Fig. 5. Transmission minimum frequency with varying number of turns in SRR.

Table 2. Calculated transmission minimum frequency and simulated frequency of SRR.

S.N.	No. of rings (N)	Length of outer ring *l* (mm)	L(nH)	C(pF)	Transmission Minimum frequency (in GHz) (calculated)	Transmission Minimum frequency (in GHz) (simulated)
1	2	4	26.267	0.0235	6.19	5.21
2	3	4.8	23.90	0.054	4.47	4.19
3	4	5.6	23.95	0.08625	3.48	3.60
4	5	6.4	24.85	0.12595	2.81	2.78
5	6	7.2	26.08	0.17105	2.36	2.37

It is evident from the results that the numerically analysed resonant frequency is nearly equal to the analytically calculated from its equivalent circuit in SRRs as well as SRs. It is also seen from the tabulated results that SR resonates at a lower frequency and low transmission minimum than the SRR of same size. Hence it is inferred that SRs have substantial potential to decrease the electrical size of MTM as compared to square SRR structures. Great coupling of incident magnetic energy can be attained by maximizing the enclosed cell area to efficiently use the cell area which is possible with SR only.

5. Conclusion

In the proposed work, we have analyzed and compared the mathematical model of equivalent circuit of the SRR and SR with varying number of rings and turns respectively, and

show that analytical results nearly match with its full-wave numerical simulations results. The error in the analytical calculated frequency and simulated frequency is less although the size of resonant particles are in millimeter range and it will further reduce if dimension are micrometer or nanometer range leading to the customized material to resonant in terahertz regime. The expressions derived for resonant frequency are modified for evaluating effective dielectric constant of substrate after incorporation of metallic inclusions. It is seen that the analytical calculated transmission minimum frequency accurately match with the full wave simulated frequency in SRR for varying number of rings and varying number of turns in SR. The use of SR is proposed in this paper as SR decreases the electrical size of MTM than square SRR structures because the small sized SR can provide same magnetic resonance as large sized SRR. It is thus deduced that a spiral resonator is a better option as it draws on less area and high package density.

References

[1] Engheta, N. 2003. Metamaterials with Negative Permittivity and Permeability: Background, Salient Features, and New Trends. *International Microwave Symposium digest*, 1: 187-190.

[2] Veselago, V.G. 1968. The Electrodynamics of Substances with Simultaneously Negative Values of ε and μ. *Soviet Physics Uspekhi*, 10(4): 509-514.

[3] Pendry J.B, Holden A.J, Robbins D.J and Stewart, W.J. 1998. Low Frequency Plasmons for Thin-Wire structure. *Journal of Physics: Condensed Matter*, 10(22): 4785–4809.

[4] Sihvola, A. 2007. Metamaterials in Electromagnetics. *Metamaterials*: *Springer*, 1: 2–11.

[5] Pendry J.B, Holden A.J, Robbins D.J and Stewart, W.J. 1999. Magnetism from conductors and enhanced nonlinear phenomena.IEEE Transactions of Microwave Theory and Technology. *IEEE Transactions of Microwave Theory and Techniques*, 47: 2075–2084.

[6] Maslovski S.I, Tretyakov S.A and Belov, P. A. 2002. Wire media with negative effective permittivity: A quasi-static model. *Microwave and Optical Technology Letters*, 35(1): 47–51.

[7] Smith D.R, Padilla W. J, Vier D.C, Nemat-Nasser S.C and Schultz, S. 2000. Composite medium with simultaneously negative permeability and permittivity. *Physical Review Letters*, 84: 4184–4187.

[8] Aydin K, Bulu I, Guven K, Kafesaki M, Soukoulis C.M and Ozbay, E. 2005. Investigation of magnetic resonances for different split-ring resonator parameters and designs. *New Journal of Physics*, 7(168): 1-15.

[9] Naqui J and Martin, F. 2014. Angular Displacement and Velocity Sensors Based on Electric-LC (ELC) Loaded Microstrip Line. *IEEE Sensor Journal*, 14: 939–940.

[10] Horestani A.K, Fumeaux C, Al-Sarawi S.F and Abbott, D. 2013. Displacement Sensor Based on Diamond-Shaped Tapered Split Ring Resonator. *IEEE Sensor Journal*, 13:1153–1160.

[11] Wu M.F, Meng F.Y and Wu, Q. 2005. A Compact Equivalent Circuit Model for the SRR Structure in Metamaterials. *Asia-Pacific Microwave Conference Proceedings*, 1, Dec. 2005.

[12] Wu B.I, Wang W, Pacheco J, Chen X, Grzegorczyk T and Kong, J.A. 2005. A study of using Metamaterial as antenna substrates to enhance gain. *Progress in Electromagnetic Research*, 51: 295-328.

[13] Baena J. D, Marques R., Medina F and Martel, J. 2004. Artificial magnetic metamaterial design by using spiral resonators. *Physical Review B*, 69: 014402–014406.

[14] Naqui J, Coromina J, Karami-Horestani A, Fumeaux C and Martín, F. 2015. Angular Displacement and Velocity Sensors Based on Coplanar Waveguides (CPWs) Loaded with S-Shaped Split Ring Resonators (S-SRR). *Sensors*, 15: 9628-9650.

[15] Rajni and Marwaha, A. 2015. Resonance characteristic and effective parameters of New Left Hand Metamaterial. *Telkomnika Indonesian Journal of Electrical Engineering*, 15(3): 497-503.

[16] Rajni and Marwaha, A. 2016. CSC-SR Structure Loaded Electrically Small Planar Antenna. *Applied Computational Electromagnetics Society Journal*, 31(5): 591-598.

[17] Sabah, C. 2010. Tunable Metamaterial Design Composed of Triangular Split Ring Resonator and Wire Strip for S- And C-Microwave Bands. *Progress in Electromagnetics Research B*, 22: 341-357.

[18] Buell K, Mosallaei H and Sarabandi, K. 2006. A substrate for small patch antennas providing tunable miniaturization factors. *IEEE Transactions on Microwave Theory and Techniques*, 54(1): 135–146.

[19] Rajni and Marwaha, A. 2015. Magnetic Resonance of Spiral Resonators. International Journal of Applied Engineering Research. *International Journal of Applied Engineering Research*, 10(13): 33291-33295.

[20] Bilotti F, Toscano A and Vegni, L. 2007. Design of Spiral and Multiple Split-Ring Resonators for the Realization of Miniaturized Metamaterial Samples. *IEEE Transactions on Antennas and Propagation*, 55(8): 2258-2267.

[21] Ellstein D, Wang B and Teo, K.H. 2012. Accurate models for Spiral Resonators. *9th European Radar Conference (EuRAD)*, Oct.-Nov. 2012, pp. 461-464.

[22] Bilotti F, Toscano A, Vegni L, Aydin K, Alici K.B and Ozbay, E. 2007. Equivalent-Circuit Models for the Design of Metamaterials Based on Artificial Magnetic Inclusions. *IEEE Transactions on Microwave Theory and Techniques*, 55(12): 2865-2873.